Scientific Journal for Damietta Faculty of Science **13**(3) 2023, 16-24
doi: 10.21608/SJDFS.2023.221623.1116
ISSN Print 2314-8594
ISSN Online 2314-8616

https://sjdfs.journals.ekb.eg/

Electrochemical Sensing of Antipyrine and its Interaction with ds-DNA Modified Electrode

Ahmed Abd-Elkader*[1]and Abd-Elgawad Radi[1]

[1]Department of Chemistry, Faculty of Science, Damietta University, 34517 Damietta, Egypt.

Received: 07 July 2023 /Accepted: 30 November 2023

* Corresponding author's E-mail: ahmedabdelkaderahmed984@gmail.com

Abstract

The interaction of antipyrine (AnP) with the double-stranded deoxyribonucleic acid of salmon sperm on a electrochemical electrode (GCE) was carefully examined using voltammetric methods.The Ultra violet-visible absorption method was used to determine the interaction of AnP and double strand DNA in solution. AnP give a single anodic peak in buffer solutions of (pH 3.5 - 9.5).AnP is oxidized in a diffusion-controlled process from a phosphate buffer solution, pH 7.The variation given by AnP through its current signals was monitored in the existance of DNA by GCE using different voltammetric techniques. Diffusion coefficient of free AnP was 3.7×10^{-6} and 2.8×10^{-7} cm^2s^{-1} for the AnP-DNA .The binding constant was calculated to be 1.5×10^5 and 1.1×10^5 M^{-1} using DPV and UV / vis Spectroscopy. AnP binds to DNA primarily by electrostatic interaction with a contribution from intercalation. A detection pattern depends on pre-concentration and DPV detection at GCE modified with dsDNA was introduced to determine AnP in saliva matrices.

Keywords: DNA reaction, antipyrine, voltammogram, uv-techniques, saliva.

Graphical abstract

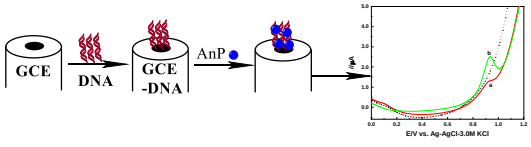

Introduction

Mites are one of the major pests that living in a

Antipyrine AnP (phenazone, 1,5-dimethyl-2-phenyl-4-pyrazone) is widely used in clinical treatment as an analgesic, antipyretic and anti-inflammatory agent. Despite its severe toxicity, it is still used to treat febrile patients as an injectable solution. A particular interest was given to antipyrine as a biomarker in testing the effects of other drugs(Marques, Takayanagui et al. 2002, Burmańczuk, Kowalski et al. 2016)or diseases(Nazareth, Rege et al. 1990) on drug-metabolizing enzymes in the liver(Fabre, Bressolle et al. 1993). In addition, AnP has been widely used as a sensor (Mahmoud, Abdel-Kader et al. 2007). In particular, the effect of

various drug and pathological conditions on hepatic P-450 enzyme activity has been of interest as a determinant of enzematic activity by observing variations of AnP clearance (Zhang, Sun et al. 2004). Sensitive and straightforward detection methods are required for rapid antipyrine monitoring. So far, several methods have been used to quantify AnP, like (HPLC) (Eichelbaum and Spannbrucker 1977, Kitzman, Martin et al. 1988), (LC–MS) (Abernethy, Greenblatt et al. 1981) , (TLC) (Welch, DeAngelis et al. 1975), and capillary electrophoresis (Perrett and Ross 1995). Most of these methods need some requirements such as complex sample pretreatment, time-consuming steps of extraction, toxic and expensive reagents, costly and complex equipments, competent subjects, and a lengthy recognition operation.Thus, these methods are not suitable for online analysis. so, a fast and highly selective technique is highly desirable. Until now, electroanalytical methods have attracted increasing attention because of the merits of inexpensive instrumentation, rapid response, time-consuming process, excellent selectivity, high sensitivity, and real-time detection under various conditions. To our knowledge, however, only a few attempts have been made to analyze Anp using electroanalytical procedures (Meng, Xu et al. 2012, Mayerhuber, Trattner et al. 2021). HPLC with electrochemical detection (ED) for the simultaneous determination of aminopyrine and antipyrine has been developed (Erkang and Jianxun 1990).

The interaction of drugs with DNA have shown much interest in monitoring small molecules such as pesticides(Morawska, Jedlińska et al. 2019), drugs(Brahman, Dar et al. 2012)and testing the nature and the factors affecting their binding mechanism. Various methods have been used to study this interactions, involving UV vis spectrophotometry(Marky, Snyder et al. 1983), fluorescence spectroscopy (Jenkins 1997), synchronous wavelength spectroscopy (CW-SFS) (Ni, Lin et al. 2008), Raman circular spectroscopy (Manfait, Alix et al. 1982). Nowadays, interest in electrochemical studies of drug-DNA interactions has increased compared to previous methods; electroanalytical methods are distinguished by their simplicity and need fewer samples, which offers merits over the widely used biological and chemical tests.

Therefore, an attempt is being carried out to join the results of electroanalytical procedures with techniques to understand the nature of the interaction of small organic molecules and DNA (Li, Ma et al. 2005). The electrochemical approach can also quantify these drugs using a modified DNA electrode (Arshad, Yunus et al. 2012). In this study, CV and DPV have explored the nature of reaction between AnP and ss dsDNA. The diffusion coefficients were determined. UV-Vis technique was also used to determine the nature of interaction. The merits of electrochemical methods include the potential for miniaturization, simple automation, and simple portable device design. In addition, the interaction of AnP and ss dsDNA on the surface of electrode was studied, and an assay method was developed to detect AnP at dsDNA-GCE biosensors.

Experimental

Apparatus

Electroanalytical measurements were accomplished using Potentiostat Autolab PGSTAT 302N controlled by NOVA 1.11 computer software. A three-electrode system consists of a glassy carbon (Φ = 3 mm diameter) as working electrode. reference electrode is an Ag/AgCl (KCl 3.0 M) (BAS model MF-2063), and platinum wire is a counter electrode was used (BAS model MW-1032), The UV measurments were done using a PerkinElmer UV-vis spectrophotometer controlled by UV WinLab PC software for data.

Reagents

AnP was purchased from Aldrich 98%. AnP solution (0.1 M) was made with anhydrous methanol and preserved in dark. Diluting working solutions was carried out useing 0.1 M phosphate buffer solutions (PBS). Chemicals were of analytical grade and were used as it is. Solutions were prepared usind deionized water. DNA Salmon sperm sodium salt from (Sigma, D-1626, USA).It is contain of , 41.2% G-C base pairs with molecular weight $\approx 1.3 \times 10^6$ Da ($\approx$ 2000 base pairs). Purity of the DNA was spectrophotometrically determine by the absorbance ratio at 260 and 280 nm, which value of about is 1.8, typical for protein-free DNA.Disodium hydrogen phosphate solution (Na_2HPO_4), o-phosphoric acid (H_3PO_4), and

sulfuric acid (H_2SO_4) were provided by Sigma-Aldrich . DNA stock solutions were prepared using PBS of (pH 7.4) and stored in the dark. The rest of the other chemicals used was analytical reagent grade. Triply distilled water was available in all solutions at room temperature (25°C).

Procedures

Bare glassy carbon electrode was prepared using 0.05 mm alumina suspension on micro-cloth pads, and rinsed with deionized water. Analysis of fixed AnP concentration were recorded in the existence of ascending concentrations of ss dsDNA in PBS (pH 7.4). CV, DPV, or UV-absorption spectra were recorded after maintaining an interaction time of 10 minutes following each addition of DNA to AnP.. DNA was bound to the electrode surface using diazonium chemistry (Radi, Muñoz-Berbel et al. 2009, Radi, Muñoz-Berbel et al. 2009). The DNA-modified electrode could either be used immediately or stored at 4°C until required. To accumulate AnP on the dsDNA-GCE, it was immersed in a buffered solution of AnP for 5 minutes at an open circuit. Following accumulation, the electrode was rinsed and placed in an AnP-free phosphate buffer solution, and CV or DPV was recorded. The proposed protocol for quantifying AnP was then utilized to examine recovery from human saliva. Saliva samples obtained from healthy subjects were frozen until analysis. To analyze the pure drug, 1.0 ml of saliva was pipetted into polypropylene bottles, which were then centrifuged at 5000 rpm for 5 minutes. The clear supernatant (500 µl) was subjected to DPV analysis.

Results and discussion

AnP interaction with DNA in solution via CV

Figure 1 displays typical CVs of AnP in the absence and presence of ss dsDNA at the GCE. AnP (curve a) exhibits a distinctive oxidation peak at 1.0 V, but no corresponding reduction peak is observed in the reversed scan from 1.0 to 0.0 V, indicating that the oxidation of AnP within the chosen potential range is an irreversible electrochemical process. Our experimental conditions demonstrate that ss-dsDNA does not exhibit faradaic reactions at potentials ranging from 0.0 to 1.2 V (curve c). Therefore, the reduction in the peak currents of AnP and the positive shift in the peak potential are due to the binding of AnP to dsDNA, as depicted in curve b.

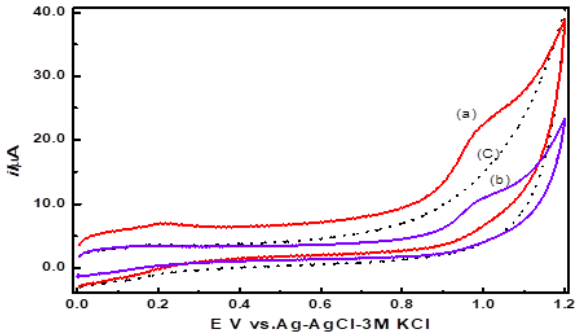

Fig 1. CVs of 1.0×10^{-4} M AnP (a) in absence and (b) presence of 5.0×10^{-4} M DNA at GCE electrode in PBS, pH 7.4, scan rate 100 mVs^{-1}, (c) 5.0×10^{-4} M DNA.

The AnP-DNA adduct exhibits a more positive peak potential than the parent AnP due to the slow electron transfer rate from the adduct compared to the parent AnP. This sluggish electron transfer from the AnP-DNA adduct makes the oxidation of the combined AnP more challenging than that of the free AnP, resulting in a higher oxidation potential. The complex interplay between the electronic states of the compound and DNA bases likely accounts for the observed difficulty in the electrochemical oxidation reaction of the adduct relative to the parent AnP. Furthermore, the impact of scan rate (ν) on the peak current (ip) of AnP before and after interaction with DNA was analyzed (Fig. 2). Both AnP and AnP-DNA adduct peak currents were found to be linearly related to the square root of scan rate ($\nu^{1/2}$), reflecting that the oxidation process was driven by the diffusion of the electroactive species to the electrode surface (Faulkner 1980).

Moreover, the reduced linear slope of the AnP-DNA adduct indicates that AnP can bind with DNA in solution to create a high molecular weight AnP-DNA adduct, which leads to a noticeable decrease in the apparent diffusion coefficient (Wang, Peng et al. 2003). For a diffusion-controlled irreversible electron transfer process, the Randles-Ševčík equation can be utilized to compute the diffusion coefficient: (D.A.C. Brownson and C.E. Banks 2014)

$$i_p^{irrev} = \pm 0.496\ (\propto n')^{\frac{1}{2}} nFAC(FD\ \ \frac{\nu}{RT})^{\frac{1}{2}} \quad (1)$$

The Randles-Ševčík equation involves several factors, including the geometric area of the electrode (A, in cm2), the transfer coefficient (α, typically assumed to be close to 0.5), the total number of electrons transferred per molecule in the electrode process (n), and the number of electrons transferred per mole in the rate-determining step (n'). For free AnP, the calculated diffusion coefficient (D_f) was 3.7×10^{-6} cm^2 s^{-1}. In contrast, the diffusion coefficient for the AnP-DNA adduct (D_b) was 2.8×10^{-7} cm^2 s^{-1}, which is approximately one-tenth of D_f. This reduction in diffusion is likely due to the binding of AnP to the bulky, slow-diffusing, high molecular weight DNA, which hinders the movement of the bound drug..

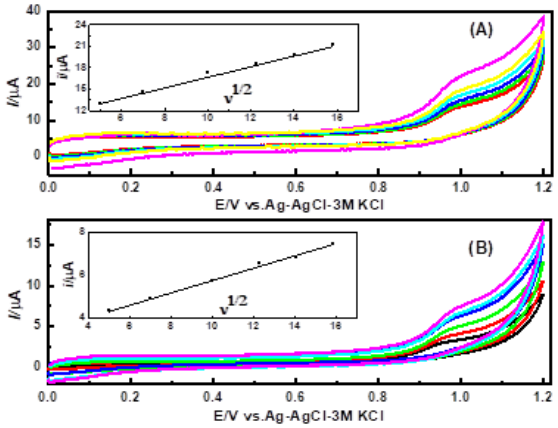

Fig 2. CVs of 1.0×10^{-4} M AnP (A) in the absence and (B) presence of 5.0×10^{-4} M DNA at GCE electrode in PBS, pH 7.4, at different scan rates (υ). Inset: ip-$\upsilon^{1/2}$ plots.

Interaction of AnP and DNA via DPV

Compared to CV, the DPV technique offers superior peak resolution and sensitivity when investigating the electrochemical behavior of biological systems. Utilizing DPV, researchers investigated the impact of pH on the electrochemical oxidation of 50 µM AnP in aqueous supporting electrolytes, spanning a pH range from 3.0 to 9.5 (as shown in Fig. 3). The anodic peak potential of AnP was observed to shift linearly towards more negative values, while the peak current increased up to a pH of 7.0. Subsequently, at pH 8.0, the peak potential and peak current remained mostly unaffected by pH, which can be attributed to modifications in the protonation of the acid-base functions within the molecule..

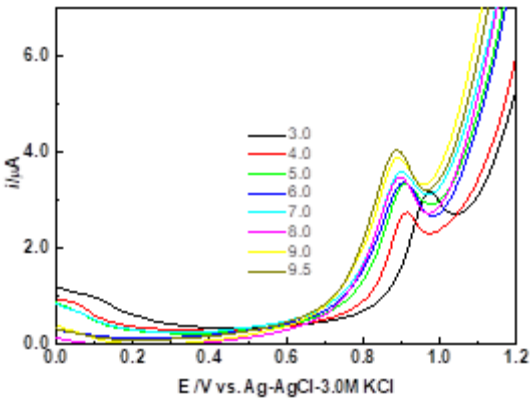

Fig 3. DPVs of 5.0×10^{-5} M AnP on GCE in PBS, at different pH values; pulse amplitude 50 mV, pulse width 30 s, sample width 0.02 s.

DPV was utilized to investigate the oxidation process of AnP in a phosphate buffer with a pH of 7.4, both in the presence and absence of DNA, as depicted in Fig. 4. By adding varying concentrations of DNA (ranging from 5.0 to 50.0µM) and observing the decrease in peak current of AnP, the binding constants (K) of AnP with DNA can be determined. The intersection of the plot of peak current versus DNA concentration allows for the calculation of the binding constant from the intersection of the plot of log (1/[DNA]) versus log $(\frac{i_a}{i_0} - i_a)$ (Fig. 4 inset) (Zhao, Zhu et al. 1999, Zia ur, Shah et al. 2009, Shujha, Shah et al. 2010):

$$\log\left(\frac{1}{[DNA]}\right) = logK_b + \log\left(\frac{i_a}{i_0} - i_a\right) \quad (2)$$

From the intercept of the linear plot of log (1/[DNA]) versus $\log\left(\frac{i_a}{i_0} - i_a\right)$ K value of 1.4×10^5 M^{-1} is obtained.

To gain a better understanding of the binding mechanism between AnP and DNA, we employed NaCl to examine the impact of ionic strength on the voltammetric behavior of AnP bound to DNA. If electrostatic binding is the primary mode of interaction between AnP and DNA, then the complex interaction should be highly sensitive to ionic strength, and significant changes in the peak anodic current of AnP would be observed over a wide range of NaCl concentrations (0.0-120 mM). Based on our findings, it can be concluded that electrostatic effects are the predominant binding mode for the interaction between AnP and DNA

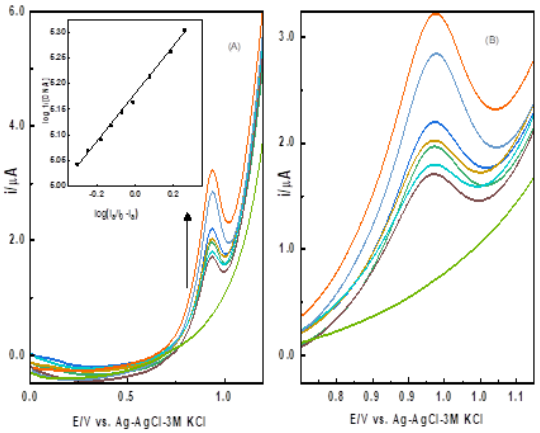

Fig 4. (A)DPVs of 5.0×10^{-5} M AnP in PBS, pH 7.4, in the presence of increasing concentrations of ss-dsDNA: (0.00- 6.0×10^{-4}) **M** at GCE. (B) the arrow shows that the current changes upon increasing DNA concentration. Inset: [1-(i_0/i_a)] versus log [1/CDNA] plot.

Absorption Spectroscopy

The binding of a drug to DNA has been classically characterized by absorption titrations (Pyle, Rehmann et al. 1989). The addition of an extrinsic compound to a given compound can result in a change in its absorption spectrum, providing an effective means of determining whether an interaction has taken place between the two compounds. In the case where the extrinsic compound is DNA, hypochromism is typically indicative of the stabilization of the DNA double helix, where intercalation or electrostatic effects are the primary binding modes. Conversely, hyperchromism can be attributed to the breakage of the DNA double helix (Shi, Guo et al. 2011).

To examine the interaction between AnP and DNA, extrinsic DNA was gradually added to a fixed concentration of 1.0 µM AnP. As depicted in Fig. 5, the absorption peaks of AnP at 255 nm and 205 nm were observed. The addition of DNA resulted in a hypochromic effect on the AnP absorption spectrum, indicating that DNA and AnP interacted with one another. Intercalation or electrostatic binding modes are likely possibilities. (Zhang, Hu et al. 2012). Based on the decrease in absorbance (hypochromic effect), the binding constant (K) was calculated according to the following equation (11) (Dang, Tong et al. 1996, Dang, Nie et al. 1998):

$$\frac{A_0}{A-A_0} = \frac{\varepsilon_f}{\varepsilon_b-\varepsilon_f} + \frac{\varepsilon_f}{\varepsilon_b-\varepsilon_f}.\frac{1}{K[DNA]} \qquad (3)$$

The binding constant (K) can be determined using the absorbance coefficients (ε_f and ε_b) and the absorbances of the free (A_0) and apparent dye (A). By plotting $A_0/(A-A_0)$ versus 1/[DNA], a binding constant of 1.8×10^5 was obtained, which is consistent with the value of K (1.4×10^5 M^{-1}) obtained from CV. The moderate coupling constant suggests electrostatic interaction, which is in line with the values obtained from the electrochemical data.

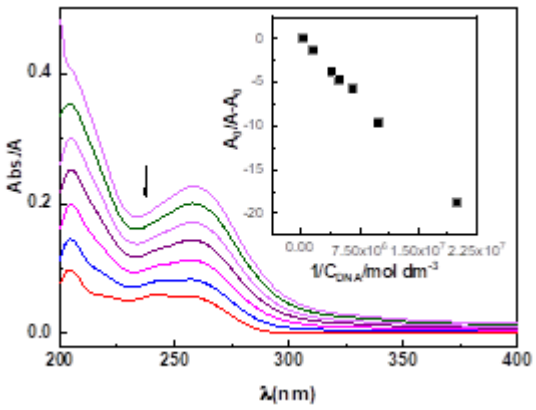

Fig 5. UV–visible absorption spectra of 5.0×10^{-5} M AnP in the presence of increasing concentrations of ss-dsDNA; 0.0-5.0×10^{-5} M in PBS, pH 7.4, Arrow shows that the absorbance changes upon increasing DNA concentration. Inset: $A_o/(A-A_o)$ vs. 1/[DNA].

AnP interaction with DNA at the electrode surface

The experiment described in the passage involves investigating the interaction between AnP and DNA at the electrode surface. Figure 6 shows the differential pulse voltammograms (DPVs) obtained for AnP in a solution, using both a bare glassy carbon electrode (GCE) and a DNA-modified GCE. When the modified electrode was immersed in the solution, voltammograms were obtained that corresponded to the oxidation of AnP. The anodic peak current generated on the DNA-modified electrode was much higher than the current generated on the bare GCE, indicating that the drug binds to the surface-confined DNA layer. This result suggests that the DNA layer on the electrode surface acts as an effective platform for the detection and quantification of AnP, potentially enabling the development of biosensors for this drug. Overall, the

experiment provides valuable insights into the interaction between AnP and DNA, and the results could potentially be useful for the development of new analytical techniques for detecting and quantifying AnP in biological samples.

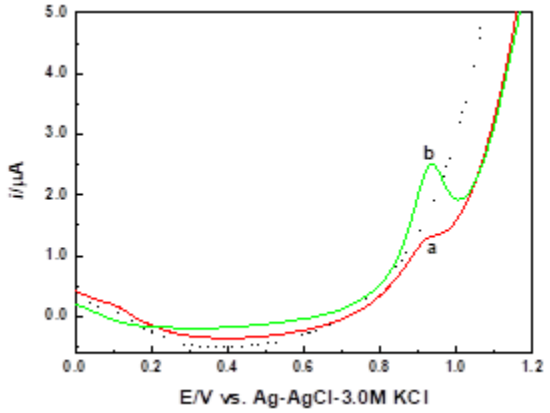

Fig 6. DPVs obtained for (a) GCE and (b) dsDNA-GCE after accumulation of AnP from 5.0×10^{-5} M AnP in PBS pH 7.4, for 5 min at open circuit, following washing of the electrode and transferred to a voltammetric cell with phosphate buffer blank solution; Other experimental conditions as in Fig.3

DPV was conducted on a DNA-modified glassy carbon electrode (DNA-GCE) using various concentrations of AnP in a phosphate buffer solution. The oxidation peak current increased with AnP concentration ranging from 0.02 to 5.0 µM, and a linear regression equation was derived as ia(µA) = (0.66 ± 0.02) + (7.89 ± 0.16) C/µmol dm³ with r = 0.998. The limit of detection (LOD) and limit of quantification (LOQ) were calculated as (3.3 /S) and (10/S), respectively.{Miller, 2018 #36;Radi, 2013 #47}, where S is the slope of the calibration curve. The calculated LOD and LOQ values were given as 2.5 and 7.5 nM, respectively. The good sensitivity of the recommended voltammetric method for AnP quantification was proved through the low LOD value.

To assess the reliability of the assay results, we conducted both intraday and interday tests with 50 nM AnP (n = 5). The low RSD value of 3.8 indicates the excellent accuracy of the method for determining AnP. The coefficients of variation around 5.2% suggest the acceptable accuracy of the electroanalytical method developed. Furthermore, we examined the reproducibility of DNA/GCE fabrication using five different electrodes, with a relative standard deviation (RSD) of 4.2%, indicating that the fabricated electrode has good reproducibility. We compared the analytical efficiency of our proposed methods for AnP determination with others, and the findings are presented in Table 1. The results demonstrate that the DNA-GCE approach achieved a wide linear range and a relatively low detection limit, indicating its potential for use in AnP detection.

Table 1 Efficiency comparison of DNA-GCE for AnP detection with other methods.

Methods	**Linear range**	**LOD**	**Ref.**
LC–MS	26.56–1062 µM	26.56 µM	(Annola, Keski-Rahkonen et al. 2008)
Capillary electrophoresis	10–350 µM	10 µM	(Perrett and Ross 1995)
LC	1.33–106.3 µM	1.33 µM	(Gurley, Zermatten et al. 1994)
HPLC	0.531–159.38 µM	0.531 µM	(Eichelbaum and Spannbrucker 1977)
GLC–NPD	5.31–265.63 µM	-	(Abernethy, Greenblatt et al. 1981)
Ion-selective electrodes for antipyrine and its derivatives			
Bi_2S_3/GCE	2–800 µM	0.7 µM	(Meng, Xu et al. 2012)
ds-DNA/GCE	0.02-5.0 µM	0.0025 µM	Thiswork

Effect of interferents

To evaluate the potential impact of various interferents, we added caffeine, paracetamol, barbital, citric acid, dopamine, uric acid, and ascorbic acid to a solution containing 5.0 µM AnP in PBS pH 7.4, tested at a concentration ratio of 10:1 to AnP, and compared it to a standard AnP solution. The obtained results demonstrated that these compounds did not significantly interfere with the proposed method, with the change in peak current being <4.5%. Therefore, our findings suggest that the DNA/GCE method has excellent selectivity for AnP and can be used to determine AnP in real samples.

Analytical application

In order to demonstrate the practical application of the DPV method, we analyzed saliva samples spiked with AnP to obtain final

concentrations ranging from 0.02 to 0.16 µM (equivalent to approximately 30.0 to 300 ng per ml of saliva), as shown in Figure 7. The samples were prepared according to the protocol outlined previously, and DPV of AnP was conducted at DNA-GCE after medium exchange. The resulting voltammograms from the saliva samples showed no extraneous peaks, and the AnP concentration was interpolated from the calibration curve. To evaluate the accuracy of the proposed method, a series of saliva samples were analyzed, and the results are summarized in Table 2. The recoveries ranged from 94.2 to 101.3%, indicating that DNA-GCE has high accuracy for determining AnP and demonstrating good recovery from saliva samples, thereby supporting the specificity of the method for AnP. Furthermore, the lowest measurable concentration of AnP in saliva was 15 ng per ml, which is lower than the concentration determined by high-performance liquid chromatography (Danhof, de Groot-van der Vis et al. 1979).

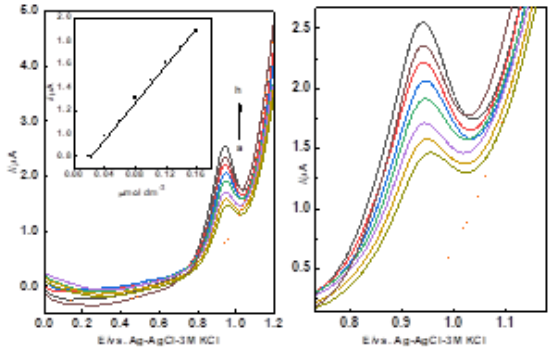

Fig 7. DPVs at the dsDNA-GCE after medium exchange for the determination of AnP in saliva samples spiked with increasing AnP concentration (a) 0.02, (b) 0.04, (c) 0.06, (d) 0.08, (e) 0.10, (f) 0.12, (g) 0.14 and (h) 0.16 µM. Dotted lines represent the blank. Other experimental conditions as in Fig.3. Inset: calibration curve.

Table 2 Results of recovery measurements of AnP in spiked saliva samples with DPV (n=3).

Added (µM)	Found (µM)	Recovery %	RSD (%)
0.02	0.0196	98.2	2.90
0.06	0.0607	101.3	1.27
0.10	0.0987	98.7	3.13
0.14	0.1319	94.2	3.81

Conclusions

The study described in the passage provides important insights into the interaction between AnP and DNA, which is a critical factor in the drug's pharmacological effects. The use of electrochemical and spectroscopic techniques allowed for a detailed analysis of the binding mechanism between AnP and DNA, revealing that AnP is bound to the DNA double helix by a combination of intercalation and electrostatic interaction with the anionic phosphate moieties. In addition, the study developed a novel DPV method using DNA-modified surfaces to quantify AnP in saliva samples. The assay showed high accuracy and good recovery from saliva samples, and it provides a practical and sensitive method for determining AnP content in clinical settings. The ability to accurately measure AnP concentrations in saliva could be useful for optimizing dosage and monitoring patient response. Overall, the study demonstrates the utility of electrochemical-based methods for studying drug-DNA interactions and provides a new assay for quantifying AnP in saliva, which could have important implications for the clinical use of this drug.

References

Abernethy, D. R., et al. (1981). "Antipyrine determination in human plasma by gas—liquid chromatography using nitrogen—phosphorus detection." Journal of Chromatography B: Biomedical Sciences and Applications **223**(2): 432-437.

Annola, K., et al. (2008). "Simultaneous determination of acrylamide, its metabolite glycidamide and antipyrine in human placental perfusion fluid and placental tissue by liquid chromatography–electrospray tandem mass spectrometry." Journal of Chromatography B **876**(2): 191-197.

Arshad, N., et al. (2012). "Electrochemical and spectroscopic investigations of isoniazide and its analogs with ds.DNA at physiological pH: evaluation of biological activities." European journal of medicinal chemistry **47**(1): 452-461.

Brahman, P., et al. (2012). "Voltammetric study of ds-DNA–flutamide interaction at carbon paste electrode." Arabian Journal of Chemistry **373**.

Burmańczuk, A., et al. (2016). "Pharmacokinetic investigations of the marker active metabolites 4-methylamino-antipyrine and 4-amino-antipyrine after intramuscular injection of metamizole in healthy piglets." Journal of Veterinary Pharmacology and Therapeutics **39**(6): 616-620.

D.A.C. Brownson and C.E. Banks (2014). The

Handbook of Graphene Electrochemistry. London, Springer London.

Dang, X.-J., et al. (1998). "Inclusion of the parent molecules of some drugs with β-cyclodextrin studied by electrochemical and spectrometric methods." Journal of Electroanalytical Chemistry **448**(1): 61-67.

Dang, X.-J., et al. (1996). "The electrochemistry of the inclusion complex of anthraquinone withβ-Cyclodextrin studied by means of OSWV." Journal of inclusion phenomena and molecular recognition in chemistry **24**(4): 275-286.

Danhof, M., et al. (1979). "Assay of antipyrine and its primary metabolites in plasma, saliva and urine by high-performance liquid chromatography and some preliminary results in man." Pharmacology **18**(4): 210-223.

Eichelbaum, M. and N. Spannbrucker (1977). "Rapid and sensitive method for the determination of antipyrine in biological fluids by high-pressure liquid chromatography." Journal of Chromatography A **140**(3): 288-292.

Erkang, W. and Z. Jianxun (1990). "Simultaneous determination of aminopyrine and antipyrine by liquid chromatography/electrochemistry with a parallel dual electrode." Microchemical Journal **42**(3): 259-266.

Fabre, D., et al. (1993). "Identification of Patients with Impaired Hepatic Drug Metabolism Using a Limited Sampling Procedure for Estimation of Phenazone (Antipyrine) Pharmacokinetic Parameters." Clinical Pharmacokinetics **24**(4): 333-343.

Faulkner, A. J. B. L. R. (1980). Electrochemical Methods: Fundamentals and Applications. New York, Wiley.

Gurley, B. J., et al. (1994). "Determination of antipyrine in human serum by direct injection restricted access media liquid chromatography." Journal of Pharmaceutical and Biomedical Analysis **12**(12): 1591-1595.

Jenkins, T. C. (1997). "Optical absorbance and fluorescence techniques for measuring DNA-drug interactions." Methods Mol Biol **90**: 195-218.

Kitzman, J. V., et al. (1988). "Determination of antipyrine in catfish plasma by high-performance liquid chromatography." Journal of Chromatography A **437**: 306-310.

Li, N., et al. (2005). "Interaction of anticancer drug mitoxantrone with DNA analyzed by electrochemical and spectroscopic methods." Biophys Chem **116**(3): 199-205.

Mahmoud, M., et al. (2007). "Antipyrine clearance in comparison to conventional liver function tests in hepatitis C virus patients." Eur J Pharmacol **569**(3): 222-227.

Manfait, M., et al. (1982). "Interaction of adriamycin with DNA as studied by resonance Raman spectroscopy." Nucleic acids research **10**(12): 3803-3816.

Marky, L. A., et al. (1983). "Thermodynamics of drug-DNA interactions." J Biomol Struct Dyn **1**(2): 487-507.

Marques, M. P., et al. (2002). "Albendazole metabolism in patients with neurocysticercosis: antipyrine as a multifunctional marker drug of cytochrome P450." Braz J Med Biol Res **35**(2): 261-269.

Mayerhuber, L., et al. (2021). "Development of ion-selective electrodes for antipyrine and its derivatives as potential tool for environmental water monitoring." Journal of Electroanalytical Chemistry **886**: 115110.

Meng, X., et al. (2012). "Electrochemical behavior of antipyrine at a Bi2S3 modified glassy carbon electrode and its determination in pharmaceutical formulations." Analytical Methods **4**(6): 1736-1741.

Miller, J. and J. C. Miller (2018). Statistics and chemometrics for analytical chemistry, Pearson education.

Morawska, K., et al. (2019). "Analysis and DNA interaction of the profluralin herbicide." Environmental Chemistry Letters **17**(3): 1359-1365.

Nazareth, H. M., et al. (1990). "Antipyrine clearance: prognostic marker for obstructive jaundice." Indian J Gastroenterol **9**(1): 63-66.

Ni, Y., et al. (2008). "Synchronous fluorescence and UV-vis spectroscopic studies of interactions between the tetracycline antibiotic, aluminium ions and DNA with the aid of the Methylene Blue dye probe." Anal Chim Acta **606**(1): 19-25.

Perrett, D. and G. A. Ross (1995). "Rapid determination of drugs in biofluids by capillary electrophoresis Measurement of antipyrine in saliva for pharmacokinetic studies." Journal of Chromatography A **700**(1): 179-186.

Pyle, A. M., et al. (1989). "Mixed-ligand complexes of ruthenium(II): factors governing binding to DNA." Journal of the American Chemical Society **111**(8): 3051-3058.

Radi, A.-E., et al. (2009). Electroanalysis **21**(6): 696-700.

Radi, A.-E., et al. (2009). "An electrochemical immunosensor for ochratoxin A based on immobilization of antibodies on diazonium-functionalized gold electrode." Electrochimica Acta **54**(8): 2180-2184.

Shi, Y., et al. (2011). "Interaction between DNA and Microcystin-LR Studied by Spectra Analysis and Atomic Force Microscopy." Biomacromolecules **12**(3): 797-803.

Shujha, S., et al. (2010). "Diorganotin(IV) derivatives of ONO tridentate Schiff base: Synthesis, crystal structure, in vitro antimicrobial, anti-leishmanial and DNA binding studies." European journal of medicinal chemistry **45**(7): 2902-2911.

Wang, S., et al. (2003). "Electrochemical determination of interaction parameters for DNA and mitoxantrone in an irreversible redox process." Biophys Chem **104**(1): 239-248.

Welch, R. M., et al. (1975). "Elimination of ntipyrine from saliva as a measure of metabolism in man." Clin Pharmacol Ther **18**(3): 249-258.

Zhang, G., et al. (2012). "Spectroscopic studies on the interaction between carbaryl and calf thymus DNA with the use of ethidium bromide as a fluorescence probe." J Photochem Photobiol B **108**: 53-61.

Zhang, L., et al. (2004). "Study of hepatic function matching between banna minipig inbred and humans." Transplantation Proceedings **36**(8): 2492-2494.

Zhao, G.-C., et al. (1999). "Voltammetric studies of the interaction of methylene blue with DNA by means of β-cyclodextrin." Anal Chim Acta **394**(2-3): 337-344.

Zia ur, R., et al. (2009). "Synthesis, characterization and DNA binding studies of penta- and hexa-coordinated diorganotin(IV) 4-(4-nitrophenyl)piperazine-1-carbodithioates." Journal of Organometallic Chemistry **694**(13): 1998-2004.

الملخص العربي

عنوان البحث: الاستشعار الكهروكيميائي للانتيبيرين وتفاعله مع الحامض النووى الديؤكسى ريبوزى للالكترود المعدل

أحمد عبد القادر*[١] ، عبد الجواد راضي[١]
[١] قسم الكيمياء، كلية العلوم، جامعة دمياط، مصر

ان تفاعل الانتيبيرين مع الحامض النووى الديؤكسى ريبوزى للحيوانات المنوية للسالمون فى المحلول وأيضا عند التثبيت على سطح الالكترود الكربونى الزجاجى قد اختبر بعناية مستخدما الطرق الفولتمترية . طرق الامتصاص الطيفية UV-vis استخدمت ايضا لدراسة تفاعل الانتيبيرين مع الحامض النووى الديؤكسى ريبوزى فى المحلول. الانتيبيرين أظهر قمة آنودية فردية باستخدام محاليل البفر الفوسفاتى ذو الاس الهيدروجينى بين ٣,٥ الى ٩,٥ . الانتيبيرين يتأكسد فى عملية التحكم الانتشارى مستخدما محلول البفر الفوسفاتى ذو الاس الهيدروجينى ٧. التنوع الذى يعطيه الانتيبيرين فى قراءات التيار سجلت فى وجود الحامض النووى الديؤكسى ريبوزى مستخدما الالكترود الكربونى الزجاجى مستخدما تقنيات الفولتاميترى الدائرى والنبض التفاضلى. معامل الانتشار للانتيبيرين الحر كان ١٠-6×3.7 -s cm2 بينما للمعقد المكون من اتحاد الانتيبيرين والحامض النووى فكان معامل الانتشار ٢,٨×١٠-٧ cm2 s-1 . ثابت الارتباط تم حسابه وكان ١,٥×١٠٥ و 105×1.1 M-1 فى الوسط ٧,٤ مستخدما فولتاميترى النبض التفاضلى والتحليل الطيفى UV/vis spectroscopy على التوالى. الانتيبيرين يتفاعل أولا مع الحامض النووى الديؤكسى ريبوزى عن طريق الجذب الكهربى مع مشاركة باندماج الانتيبيرين داخل الحامض النووى الديؤكسى ريبوزى. تم استخدام فولتاميترى النبض التفاضلى للكشف عن الانتيبيرين فى عينات اللعاب باستخدام الالكترود الكربونى الزجاجى المعدل باستخدام الحامض النووى الديؤكسى ريبوزى.